

**Please cite the Published Version**

Yap, Moi Hoon, Goyal, Manu, Osman, Fatima M, Martí, Robert, Denton, Erika, Juetter, Arne and Zwigelaar, Reyer (2018) Breast ultrasound lesions recognition: end-to-end deep learning approaches. *Journal of Medical Imaging*, 6 (1). 011007. ISSN 2329-4302

**DOI:** <https://doi.org/10.1117/1.jmi.6.1.011007>

**Publisher:** SPIE - International Society for Optical Engineering

**Version:** Accepted Version

**Downloaded from:** <https://e-space.mmu.ac.uk/621716/>

**Usage rights:** © In Copyright

**Additional Information:** This is an Author Accepted Manuscript of a paper accepted for publication in *Journal of Medical Imaging*, published by and copyright SPIE.

**Enquiries:**

If you have questions about this document, contact [openresearch@mmu.ac.uk](mailto:openresearch@mmu.ac.uk). Please include the URL of the record in e-space. If you believe that your, or a third party's rights have been compromised through this document please see our Take Down policy (available from <https://www.mmu.ac.uk/library/using-the-library/policies-and-guidelines>)

## **Author Copy**

### **Citation format:**

Moi Hoon Yap, Manu Goyal, Fatima M. Osman, Robert Martí, Erika Denton, Arne Juetten, Reyer Zwiggelaar, "Breast ultrasound lesions recognition: end-to-end deep learning approaches," *J. Med. Imag.* **6**(1), 011007 (2019),  
doi: 10.1117/1.JMI.6.1.011007.

### **Copyright notice format:**

Copyright 2018 Society of Photo-Optical Instrumentation Engineers. One print or electronic copy may be made for personal use only. Systematic reproduction and distribution, duplication of any material in this paper for a fee or for commercial purposes, or modification of the content of the paper are prohibited.

# 1 Breast Ultrasound Lesions Recognition: End-to-end Deep Learning 2 Approaches

3 **Moi Hoon Yap<sup>a, \*</sup>, Manu Goyal<sup>a</sup>, Fatima Osman<sup>b</sup>, Robert Martí<sup>c</sup>, Erika Denton<sup>d</sup>, Arne  
4 Juette<sup>d</sup>, Reyer Zwiggelaar<sup>e</sup>**

5 <sup>a</sup>Manchester Metropolitan University, Faculty of Science and Engineering, School of Computing, Mathematics and  
6 Digital Technology, Chester Street, Manchester, UK, M14 6TE

7 <sup>b</sup>Department of Computer Science, Sudan University of Science and Technology, Khartoum, Sudan.

8 <sup>c</sup>Computer Vision and Robotics Institute, University of Girona, Spain

9 <sup>d</sup>Norfolk and Norwich University Hospital Foundation Trust, Norwich, UK

10 <sup>e</sup>Aberystwyth University, Department of Computer Science, Aberystwyth, SY23 3DB, UK

11 **Abstract.** Multi-stage processing of automated breast ultrasound lesions recognition is dependent on the performance  
12 of prior stages. To improve the current state of the art, we propose the use of end-to-end deep learning approaches  
13 using Fully Convolutional Networks (FCNs), namely FCN-AlexNet, FCN-32s, FCN-16s and FCN-8s for semantic  
14 segmentation of breast lesions. We use pre-trained models based on ImageNet and transfer learning to overcome the  
15 issue of data deficiency. We evaluate our results on two datasets, which consist of a total of 113 malignant and 356  
16 benign lesions. To assess the performance, we conduct 5-fold cross validation using the following split: 70% for  
17 training data, 10% for validation data, and 20% testing data. The results showed that our proposed method performed  
18 better on benign lesions, with a top *Mean Dice* score of 0.7626 with FCN-16s, when compared to the malignant  
19 lesions with a top *Mean Dice* score of 0.5484 with FCN-8s. When considering the number of images with *Dice*  
20 score  $> 0.5$ , 89.6% of the benign lesions were successfully segmented and correctly recognised, while 60.6% of the  
21 malignant lesions were successfully segmented and correctly recognised. We conclude the paper by addressing the  
22 future challenges of the work.

23 **Keywords:** breast ultrasound, breast lesions recognition, fully convolutional network, semantic segmentation.

24 \*Moi Hoon Yap, [m.yap@mmu.ac.uk](mailto:m.yap@mmu.ac.uk)

## 25 1 Introduction

26 Breast cancer is the most common cancer in the UK [1], where one in eight women will be di-  
27 agnosed with breast cancer in their lifetime and one person is diagnosed every 10 minutes [1].

28 Over recent years, there has been significant research into using different image modalities [2] and  
29 technical methods have been developed [3, 4] to aid early detection and diagnosis of the disease.

30 These efforts have led to further research challenge and demand for robust computerised methods  
31 for cancer detection.

32 Two view mammography is known as the gold standard for breast cancer diagnosis [2]. How-  
33 ever, ultrasound is the standard complementary modality to increase the accuracy of diagnosis.

34 Other alternatives include tomography and magnetic resonance, however, ultrasound is the most  
35 widely available option and widely used in clinical practice [5].

36 Conventional computerised methods in breast ultrasound cancer diagnosis comprised multi-  
37 ple stages, including pre-processing, detection of the region of interest (ROI), segmentation and  
38 classification [6–8]. These processes rely on hand-crafted features including descriptions in the  
39 spatial domain (texture information, shape and edge descriptors) and frequency domain. With the  
40 advancement of deep learning methods, we can detect and recognise objects without the need for  
41 hand-crafted features. This paper presents the limitation of the state of the art and conducts a fea-  
42 sibility study on the use of a deep learning approach as an end-to-end solution for fully automated  
43 breast lesion recognition in ultrasound images.

44 Two-Dimensional (2D) breast ultrasound lesion segmentation is a challenging task due to the  
45 speckle noise and being operator dependent. So far, image processing and conventional machine  
46 learning methods are deemed as preferable methods to segment the breast ultrasound lesions [9].  
47 These are dependent on the human designed features such as texture descriptors [10, 11] and shape  
48 descriptors [7]. With the help of these extracted features, image processing algorithms [12] are  
49 used to locate and segment the lesions. Some of the state-of-the-art segmentation solutions consist  
50 of multiple stages [13, 14] - preprocessing or denoising stage, initial lesion detection stage to iden-  
51 tify a region of interest [15] and segmentation [16]. Recently, Huang et al. [9] reviewed the breast  
52 ultrasound image segmentation solutions proposed in the past decade. In their study, they found  
53 that due to the ultrasound artifacts and to the lack of publicly available datasets for assessing the  
54 performance of the state-of-the-art algorithms, the breast ultrasound segmentation is still an open  
55 and challenging problem.

## 56 **2 Related Work**

57 This section summarises the state-of-the-art segmentation and classification approaches for breast  
58 ultrasound cancer analysis.

### 59 *2.1 BUS Segmentation Approaches*

60 Achieving an accurate segmentation in BUS images is considered to be a big challenge [17], be-  
61 cause of the appearance of sonographic tumors [18, 19], the speckle noise, the low image contrast,  
62 and the local changes of image intensity [20]. Considering radiologist interaction within the seg-  
63 mentation process, it could have semi-automatic or fully automatic segmentation approaches [21].

64 Semi-automated segmentation approaches require an interaction with the user such as setting  
65 seeds, specifying an initial boundary or a region of interest (ROI). For instance, in [22], a com-  
66 puterized segmentation method for breast lesions on ultrasound images was proposed. First, a  
67 contrast-limited adaptive histogram equalization was applied. Then, in order to enhance lesion  
68 boundary and remove speckle noise, an anisotropic diffusion filter was applied, guided by texture  
69 descriptors derived from a set of Gabor filters. Further, the derived filtered image was multiplied by  
70 a constraint Gaussian function, to eliminate the distant pixels that do not belong to the lesion. To  
71 create potential lesion boundaries, a marker-controlled watershed transformation algorithm was  
72 applied. Finally, the lesion contour was determined by evaluating the average radial derivative  
73 function.

74 In order to segment ultrasonic breast lesions, Gao et.al. [18] proposed a variant of a normal-  
75 ized cut (NCut) algorithm that was based on homogeneous patches (HP-NCut) in 2012. Further,  
76 HPs were spread within the same tissue HP region, which is more reliable to distinguish the different  
77 tissues for better segmentation. Finally in the segmentation stage, they used the NCut framework

78 by considering the fuzzy distribution of textons within HPs as final image features. More recently,  
79 Prabhakar et.al. [23] developed algorithm for an automatic segmentation and classification of  
80 breast lesions from ultrasound images. As a pre-processing step, speckle noise was removed us-  
81 ing the Tetrolet filter and, subsequently, active contour models based on statistical features were  
82 applied to obtain an automatic segmentation. For the classification of breast lesions, a total of  
83 40 features were extracted from the images, such as textural, morphological and fractal features.  
84 Support Vector Machines (SVM) with a polynomial kernel for the combination of texture, optimal  
85 features were used to classify the lesions from BUS images.

86 Fully automatic segmentation needs no user intervention at all. In [24], instead of using a  
87 term-by-term translation of diagnostic rules on intensity and texture, a novel algorithm to achieve  
88 a comprehensive decision upon these rules was proposed. This was achieved by incorporating im-  
89 age over-segmentation and lesion detection in a pairwise conditional random field (CRF) model.  
90 In order to propagate object-level cues to segments, multiple detection hypotheses were used. Fur-  
91 ther, a unified classifier was trained based on the concatenated features. This algorithm could avoid  
92 the limitations of bottom-up segmentation, and capable to handle very complicated cases. In the  
93 same year, a novel algorithm was proposed [19], making no assumptions about lesions, in which  
94 a hierarchical over-segmentation framework was used for collecting heterogeneous features. Con-  
95 sidering multiscale property, the superpixels were classified with their confidences nested into the  
96 bottom layer. An efficient CRF model was used for making the ultimate segmentation. Compared  
97 with other two different approaches, Hao et.al [19] algorithm was superior in performance, and  
98 was able to handle all kinds of tumors (benign and malignant).

99 In [25], two new concepts of neutrosophic subset and neutrosophic connectedness (neutro-  
100 connectedness) were defined to generalize the fuzzy subset and fuzzy connectedness. The newly

101 proposed neutro-connectedness models the inherent uncertainty and indeterminacy of the spatial  
102 topological properties of the image. The proposed method was applied to a BUS dataset with 131  
103 cases, and its performance was evaluated using the similarity ratio, false positive ratio and average  
104 Hausdroff error. In comparison with the fuzzy connectedness segmentation method, the proposed  
105 method was more accurate and robust in segmenting tumors in BUS images.

## 106 *2.2 BUS Classification Approaches*

107 The majority of state-of-the-art methods are multi-stage. First to detect a lesion, i.e. where a lesion  
108 is localised on the image [26]. The localisation of a lesion can be done by manual annotation or  
109 using automated lesion detection approaches [6, 15]. Subsequently, next step is to identify the le-  
110 sion type using feature descriptors. Amongst different proposed approaches considering solid mass  
111 classification, there are two main feature descriptors [27], i.e. echo texture [28] [11] and shape and  
112 margin features [29]. We present a couple of works on multi-stage machine learning methods. For  
113 a full review, please refer to Cheng et al. [26]. Liu et al. [30] proposed a novel breast classification  
114 system for Color Doppler flow imaging and B-Mode ultrasound. In order to obtain features from  
115 B-Mode ultrasound, many feature extraction methods were used to provide both the texture and  
116 geometric features. The first stage was an extraction of color Doppler features, which was achieved  
117 by applying blood flow velocity analysis to Doppler signals to extract several spectrum features.  
118 In addition, the authors proposed a velocity coherent vector method. Furthermore, using a sup-  
119 port vector machine classifier, selected features were used to classify breast lesions into benign or  
120 malignant classes. They achieved an area under the ROC curve of 0.9455 when validated on 105  
121 cases with 50 benign and 55 malignant. In the same year, Yap et al. [31] carried out a compre-  
122 hensive analysis of the best feature descriptors and classifiers for breast ultrasound classification.

123 They experimented with 19 features (texture, shape and edge), 22 feature selection methods and  
124 ten classifiers. From their findings, the best combination was the feature set of 4 shape descrip-  
125 tors, 1 edge descriptor and 3 texture descriptors using a Radial Basis Function Network, with an  
126 area under the ROC curve of 0.948. In 2016, Yap and Yap [32] conducted study to evaluate the  
127 performance of machine learning on human delineation and computer method. They found that  
128 there were no significant differences for benign lesions but computer segmentation showed better  
129 accuracy for malignant lesion classification.

130 There is increasing interest in deep learning for medical imaging [33] and two research groups  
131 have been successful in using this in breast ultrasound. In 2016, Huynh et al. [34] proposed the use  
132 of a transfer learning approach for ultrasound breast images classification. The authors used 1125  
133 cases and 2393 regions of interest for their experiment, where the ROIs were selected and labeled  
134 by the experts. To compare with the hand-crafted features, CNN was used to extract the features.  
135 When classify the CNN-extracted features with support vector machine on the recognition task of  
136 benign and malignant, they achieved an area under the ROC curve of 0.88. However, their solution  
137 was multi-stage and they did not share their dataset. In 2017, Yap et al. [35] demonstrated the  
138 use of deep learning for breast lesions detection, which outperformed the previous state-of-the-art  
139 image processing and conventional machine learning methods. They achieved an F-measure of  
140 0.92 on breast lesions detection and made one of the dataset available for research purposes.

141 Recently, Yap et al. [36] demonstrated the practicality and feasibility of using a deep learning  
142 approach for automated semantic segmentation for BUS lesion recognition. However, they only  
143 performed one fold validation using one type of FCNs, i.e. FCN-AlexNet. This paper extends  
144 Yap et al. [36] to 5-fold cross validation on four types of FCNs, namely, FCN-AlexNet, FCN-32s,  
145 FCN-16s and FCN-8s. We are the first to implement semantic segmentation on BUS images.



### 146 **3 Methodology**

147 This section provides an overview of the breast ultrasound datasets, the preparation of the ground  
148 truth labeling, the proposed method and the type of performance metrics used to validate our  
149 results.

#### 150 *3.1 Datasets*

151 To date, data deficiency in medical imaging analysis is a common problem. To form a larger  
152 dataset, we combined two datasets, which were the only two datasets made available for re-  
153 searchers. We provide a summary for each dataset and the details can be found in [35].

154 In 2001, a professional didactic media file for breast imaging specialists [37] was made avail-  
155 able. It was obtained with B&K Medical Panther 2002 and B&K Medical Hawk 2102 US systems  
156 with an 8-12 MHz linear array transducer. Dataset A consists of 306 images from different cases  
157 with a mean image size of  $377 \times 396$  pixels. From these images, 306 contained one or more lesions.  
158 Within the lesion images, 60 images presented malignant masses (as in Fig. 1 first row (a)) and  
159 246 were benign lesions (as in Fig. 1 first row (b)). To obtain Dataset A, the user needs to purchase  
160 the didactic media file from Prapavesis et al. [37]. Yap et al. [35] named it as Dataset A in their  
161 description.

162 In 2012, the UDIAT Diagnostic Centre of the Parc Taulí Corporation, Sabadell (Spain) has col-  
163 lected Dataset B with a Siemens ACUSON Sequoia C512 system 17L5 HD linear array transducer  
164 (8.5 MHz). The dataset consists of 163 images from different women with a mean image size of  
165  $760 \times 570$  pixels, where the images presented one or more lesions. Within the 163 lesion images,  
166 53 were malignant lesions (as in Fig. 1 first row (c)) and 110 with benign lesions (as in Fig. 1

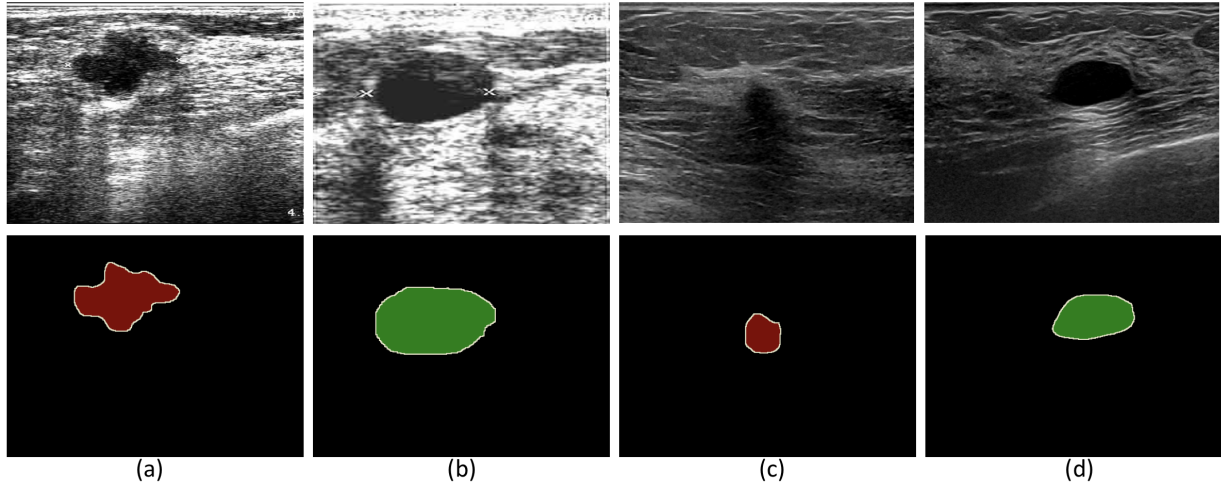


**Fig 1** Illustration of some images from the datasets and its ground truth labeling in PASCAL-VOC format.(a) and (b) are images from Dataset A; (c) and (d) are images from Dataset B; and index 1 (RED) indicates malignant lesion and index 2 (GREEN) indicates benign lesion.

167 first row (d)). Dataset B and the respective delineation of the breast lesions are available online for  
 168 research purposes, please refer to [35], where they named it as Dataset B in their description.

### 169 3.2 Ground Truth

170 Since deep learning models for semantic segmentation are widely evaluated for the PASCAL-  
 171 VOC 2012 training and validation dataset, these trained models are tested for various performance  
 172 metrics on the PASCAL-VOC 2012 test set [38, 39]. In the PASCAL-VOC 2012 dataset, the RGB  
 173 images are used as input images. The dimensions of both input images and label images should be  
 174 the same size [40]. Although the images used in training are not required to be the same size for  
 175 deep learning models in segmentation tasks, all the images are required to be of same size due to  
 176 the use of fully connected layers in these models. In the labelled image, every pixel value for each  
 177 class is an index ranging from 0 to 255. In the PASCAL-VOC 2012 dataset, there are a total of  
 178 21 classes used so far, hence, 21 indexes are used for labelling the images. For breast ultrasound  
 179 images, the format in digital media is generally grayscale. Hence, to make this compatible with the

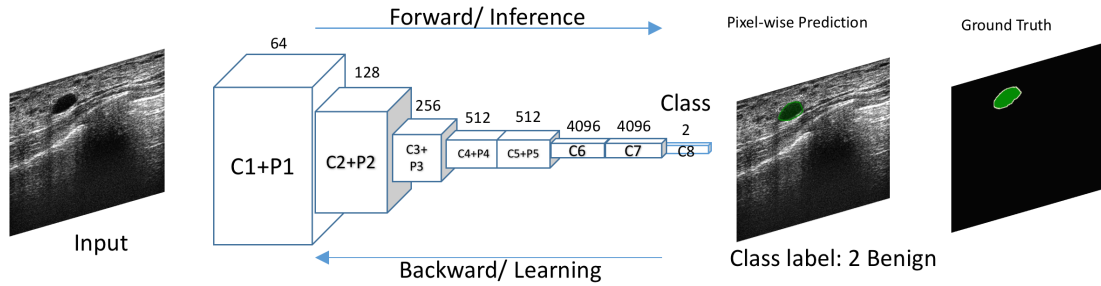


Fig 2 Overview of the semantic segmentation architecture.

180 pre-trained models and networks that are trained for PASCAL-VOC 2012 dataset (RGB images),  
 181 we converted the grayscale images to RGB images with the help of channel conversion. The  
 182 ground truths in binary masks format are converted into the 8-bit paletted label images. Fig. 1  
 183 illustrates the breast ultrasound images with the corresponding ground truth labeling in PASCAL-  
 184 VOC format, where index 1 (RED) indicates malignant lesion and index 2 (GREEN) indicates  
 185 benign lesion.

### 186 3.3 Deep Learning Framework

187 The deep learning methods proved its superiority over image processing methods and traditional  
 188 machine learning in the detection of abnormalities in medical imaging of various modalities [35,  
 189 41]. There are two main types of tasks associated with medical imaging i.e. classification and  
 190 semantic segmentation [42,43]. However, a known limitation of the classification is its inability to  
 191 locate the abnormalities in medical imaging. Hence, semantic segmentation deep learning methods  
 192 address this issues by classifying each pixel of the medical images rather than single prediction per  
 193 image in the classification task. A popular group of deep learning methods for end-to-end semantic  
 194 segmentation are fully convolutional networks (FCNs) [44].

195 FCN-AlexNet is a FCN version of the original AlexNet classification model with a few ad-  
 196 justments in the network layers for the segmentation task [44]. This network was originally used

197 for the classification of 1000 different objects of classes on the ImageNet dataset [45]. FCN-32s,  
198 FCN-16s, and FCN-8s are three models inspired by the VGG-16 based net which is a 16-layer  
199 CNN architecture that participated in the ImageNet Challenge 2014 and secured the first position  
200 in localization and second place in classification competition. All deep learning frameworks rely  
201 on feature extraction through the convolution layers, but classification networks throw away the  
202 spatial information in the fully connected layers. In contrast with classification network which  
203 ignores spatial information using fully connected layers, FCN incorporates this information by  
204 replacing fully connected layers with convolution layers. Feature maps from those convolution  
205 layers are later used for classifying each pixel to get the semantic segmentation.

206       Transfer Learning is a procedure where a CNN is trained to learn features for a broad domain  
207 after which layers of the CNN are fine-tuned to learn features of a more specific domain. Under  
208 this setting, the features and the network parameters are transferred from the broad domain to  
209 the specific one depending on several factors such as size of the new dataset and similarity to  
210 the original dataset. The use of deep learning methods for semantic segmentation in medical  
211 imaging suffer from the problem of data deficiency, which can be overcome with the help of  
212 transfer learning approaches [41,42]. In this work, the pre-trained models on the ImageNet dataset  
213 which contains more than 1.5 millions images of 1000 classes was used for transfer learning [45].  
214 The weights trained on ImageNet dataset are transferred for semantic segmentation of BUS with  
215 minor adjustments in the convolutionized fully connected layers [44]. We initialised the weights  
216 of convolutional layers from these pre-trained models rather than setting up the random weights  
217 for the limited medical datasets such as BUS dataset. Otherwise, it is very hard to converge the  
218 models based on the limited medical datasets. Hence, we fine-tuned these models by using pre-  
219 trained models and training on two classes i.e. benign and malignant in the BUS dataset as shown

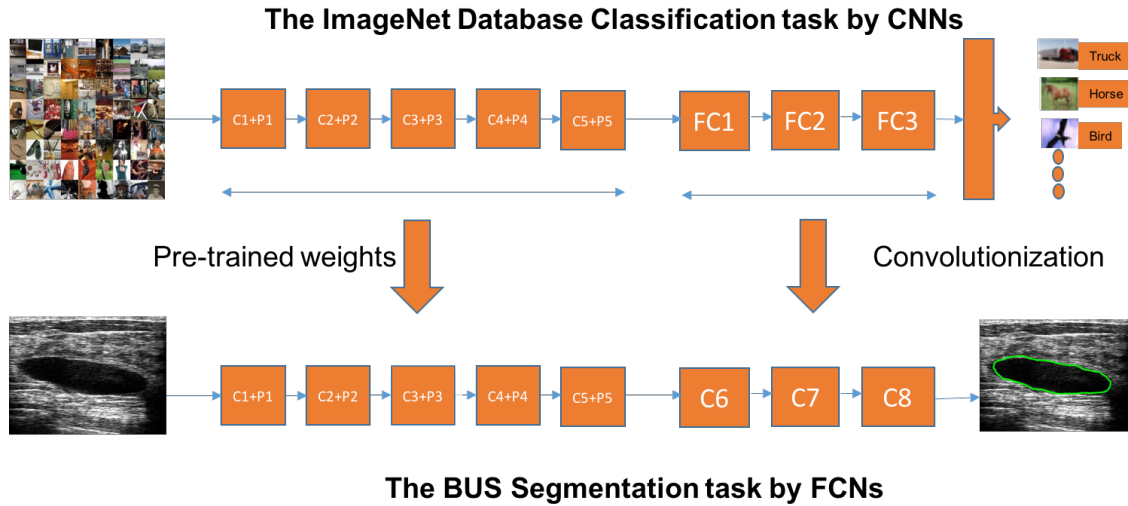


**Fig 3** Transfer learning procedure of deep CNNs to obtain optimized weights initializations. Three fully connected layers of CNN were removed and replaced by three convolutional layers, making the pre-trained model fully convolutional.

220 in the Fig. 3.

221 The combination of Dataset A and Dataset B forms a larger dataset with a total of 113 malignant  
 222 lesions and 356 benign lesions. We used the combined dataset to form better training and transfer  
 223 learning to overcome the problem of data deficiency. We used DIGITS V5 which acts as a wrapper  
 224 for the deep learning Caffe framework on the GPU machine of the following configuration: (1)  
 225 Hardware: CPU - Intel i7-6700 @ 4.00Ghz, GPU - NVIDIA TITAN X 12Gb, RAM - 32Gb DDR5  
 226 (2) Deep Learning Framework: Caffe [46].

227 We assessed the performance of the model using 5-fold cross validation using the following  
 228 split: 70% for training data, 10% for validation data, and 20% testing data. We trained the model  
 229 using stochastic gradient descent with a learning rate of 0.0001, 60 epochs with a dropout rate of  
 230 33%. The number of epochs was kept at 60 as in [47] where convergence has already happened  
 231 when we performed the empirical experiments. Fig. 2 illustrates the process of the end-to-end  
 232 solution using semantic segmentation.

**Table 1** Summary of the performances for different lesion types for four semantic segmentation methods in *Mean. SD* is standard deviation.

Lesion Type	Method	Sensitivity <i>Mean±SD</i>	Precision <i>Mean±SD</i>	Dice <i>Mean±SD</i>	MCC <i>Mean±SD</i>
Benign	FCN-AlexNet	0.8000±0.2404	0.7282±0.2191	0.7199±0.1964	0.7304±0.1762
	FCN-32s	0.8271±0.2250	0.7471±0.1923	0.7473±0.1896	0.7554±0.1689
	FCN-16s	<b>0.8374±0.2392</b>	0.7674±0.1953	<b>0.7626±0.2095</b>	<b>0.7733±0.1857</b>
	FCN-8s	0.8092±0.2683	<b>0.7940±0.1960</b>	0.7564±0.2373	0.7659±0.2172
Malignant	FCN-AlexNet	0.4708±0.3078	0.7599±0.2364	0.4894±0.2757	0.5080±0.2488
	FCN-32s	0.4492±0.2983	<b>0.7737±0.2925</b>	0.3267±0.2870	0.4001±0.2577
	FCN-16s	0.3790±0.2978	0.7481±0.2718	0.4212±0.2804	0.4616±0.2527
	FCN-8s	<b>0.5696±0.3350</b>	0.7044±0.2528	<b>0.5484±0.2785</b>	<b>0.5842±0.2358</b>

### 233 3.4 Evaluation criteria

234 Even though the method is an end-to-end solution, we evaluated the results using standard perfor-  
 235 mance metrics from the literature. To measure the accuracy of the segmentation results, the *Dice*  
 236 *Similarity Coefficient (Dice)* (henceforth *Dice*) [48, 49] was used. We report our findings in *Dice*,  
 237 *Sensitivity*, *Precision* and *Matthew Correlation Coefficient (MCC)* [50] as our evaluation metrics.

## 238 4 Results and Discussion

239 Table 1 summarises the performance of our proposed methods on benign and malignant lesions.  
 240 Overall, all the methods performed better on benign lesions, with a top *Dice* score of 0.7626,  
 241 compared to the malignant lesions with a top *Dice* score of 0.5484. The results showed that the  
 242 performance of the proposed method was dependent on the size of the dataset. In our datasets,  
 243 we have more benign images (356) than malignant images (113). Overall, FCN-16s has the best  
 244 performance in benign lesions recognition that achieved 0.8374 in *Sensitivity*, 0.7626 in *Dice Score*  
 245 and 0.7733 in *MCC*. FCN-8s has the best *Precision* of 0.7940. For Malignant lesions, FCN-8s is  
 246 the best method with 0.5696 in *Sensitivity*, 0.5484 in *Dice* and 0.5842 in *MCC*.

247 According to Everingham et al. [51], the results with *Dice* score  $> 0.5$  is considered correct de-  
 248 tection. Fig. 4 compares the performances of the proposed methods when considering the number

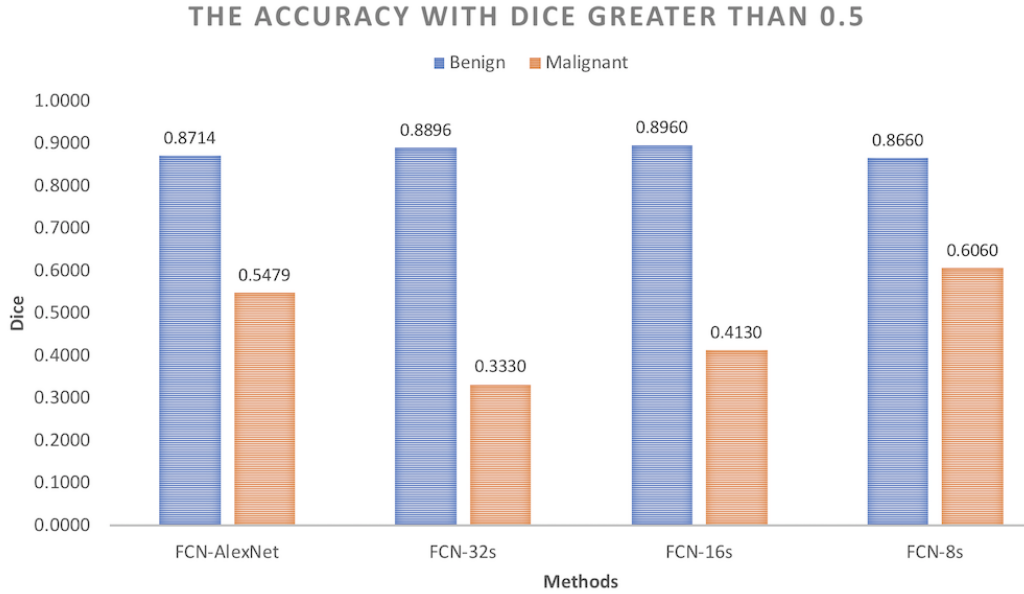


**Fig 4** The accuracy of the proposed methods when considering the number of images with *Dice* score  $> 0.5$ .

249 of images with *Dice* score  $> 0.5$ . Overall, benign lesions had higher *Dice* score, with top accuracy  
 250 of 0.8960 for FCN-16s. This implies that 89.6% of the benign lesions were successfully segmented  
 251 and correctly recognised. The results were comparable across four different methods. For malig-  
 252 nant lesions, the top accuracy is 0.6060 with FCN-8s, where only 60.6% of the malignant lesions  
 253 were successfully segmented and correctly recognised. The worst performance in malignant le-  
 254 sions recognition was FCN-32s, where only 33.3% of the lesions was successfully segmented and  
 255 recognised. *The poor performances were due to data deficiency in malignant class, which is a*  
 256 *common issue for deep learning approaches.*

257 To further illustrate the results, we visually compared the segmented regions for the proposed  
 258 methods. Four examples of the successful and failed cases for our experiment are illustrated in Fig.  
 259 5. The first row is a benign lesion, where the lesion is well-defined with clear boundaries. All the  
 260 methods achieved high *Dice* score. Fig. 5 second row illustrates a malignant lesion with irregular  
 261 boundaries and ill-defined shape. We observed that all the methods had classified the lesion to the

262 correct class. However, only FCN-16s managed to produce the closest segment when compared to  
263 the ground truth. The third row of Fig. 5 shows a benign lesion where all the methods failed to  
264 segment the lesion. This is due to the appearance of fibroadenoma are less hypo-echoic and poor  
265 image quality. The final row illustrates that even though the methods are able to segment the lesion,  
266 misclassification is an issue where FCN-AlexNet and FCN-32s have classified the hypo-echoic  
267 region as benign. FCN-8s are able to classify the lesion correctly however it also detected some  
268 benign regions within the lesion. Overall, the lesions with small area, ambiguity in the boundary  
269 and irregular shape are harder for semantic segmentation due to the lack of data to represent these  
270 categories.

## 271 **5 Conclusion**

272 The common problem in conventional machine learning are: 1) It is based on hand-crafted features;  
273 2) In some cases, it requires human intervention where the radiologists has to select the ROI; and 3)  
274 It is multi-stage and there is dependency from one stage to the next. In this paper, the problem was  
275 solved by using a deep learning approach where we have shown four types of FCNs in designing a  
276 robust end-to-end solution for breast ultrasound lesions recognition.

277 Conventional methods classified the lesion into single type, but using semantic segmentation,  
278 we observed that it is not necessarily the case. In one lesion, as illustrated in Fig. 5 row 3 and row  
279 4, it may have malignant tissue and benign tissue. This is an interesting finding for future research  
280 in understanding the tumour from both the computer vision and clinical perspectives.

281 This paper has provided a new insight for future research to by investigating four types of deep  
282 learning techniques. However, proposing an accurate end-to-end solution for breast ultrasound  
283 lesions recognition remains a challenge due to the lack of datasets to provide sufficient data repre-



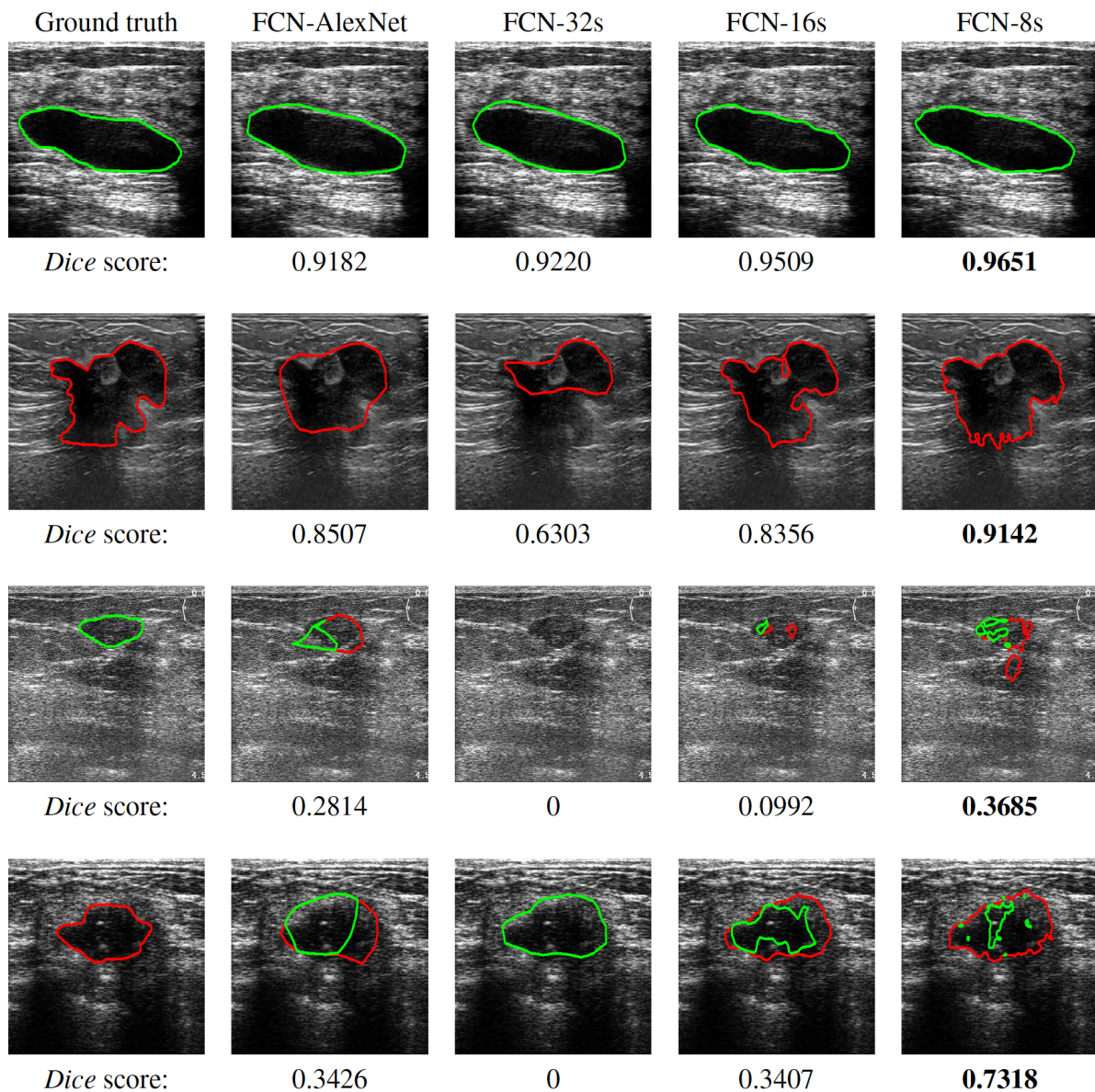


**Fig 5** Visual comparison of the lesions segmentation and recognition with FCNs. The first column is the ground truth delineation, the second column is the proposed transfer learning FCN-AlexNet, the third column is the proposed transfer learning FCN-32s and the fourth column is the proposed transfer learning FCN-16s and the last column is the proposed transfer learning FCN-8s. The first and second rows showed the best case scenarios where the lesions were correctly segmented and classified. The third and fourth rows showed difficult cases where FCNs failed in those cases.

284 sentation. In the future, with the growth of big data and data sharing efforts, an end-to-end solution  
285 based on deep learning approach may find wide applications in breast ultrasound computer aided  
286 diagnosis.

### 287 *Disclosures*

288 No conflicts of interest, financial or otherwise, are declared by the authors.

### 289 *Acknowledgments*

290 The authors would like to thank Prapavesis et al. (breast imaging specialists) [37] for providing  
291 Dataset A for this research.

### 292 *References*

- 293 1 “Breast cancer care: Facts and statistics 2017.” Online.  
294 [https://www.breastcancercare.org.uk/about-us/media/press-pack-breast-cancer-awareness-](https://www.breastcancercare.org.uk/about-us/media/press-pack-breast-cancer-awareness-month/facts-statistics)  
295 [month/facts-statistics](https://www.breastcancercare.org.uk/about-us/media/press-pack-breast-cancer-awareness-month/facts-statistics) (2017).
- 296 2 W. Berg, L. Gutierrez, M. NessAiver, *et al.*, “Diagnostic accuracy of mammography, clinical  
297 examination, US, and MR imaging in preoperative assessment of breast cancer,” *Radiology*  
298 **233**(3), 830–849 (2004).
- 299 3 M. H. Yap, A. G. Gale, and H. J. Scott, “Generic infrastructure for medical informatics (gimi):  
300 the development of a mammographic training system,” in *International Workshop on Digital*  
301 *Mammography*, 577–584, Springer (2008).
- 302 4 M. H. Yap, E. Edirisinghe, and H. Bez, “Processed images in human perception: A case study  
303 in ultrasound breast imaging,” *European Journal of Radiology* **73**(3), 682–687 (2010).
- 304 5 A. Stavros, C. Rapp, and S. Parker, *Breast Ultrasound*, 978-0397516247, LWW, 1 ed. (1995).

- 305 6 K. Drukker, M. L. Giger, C. J. Vyborny, *et al.*, “Computerized detection and classification of  
306 cancer on breast ultrasound,” *Academic Radiology* **11**(5), 526–535 (2004).
- 307 7 M. H. Yap, E. Edirisinghe, and H. Bez, “A comparative study in ultrasound breast imaging  
308 classification,” *Proc.SPIE* **7259**, 7259 – 7259 – 11 (2009).
- 309 8 J. Shan, H. Cheng, and Y. Wang, “A novel automatic seed point selection algorithm for breast  
310 ultrasound images,” in *Pattern Recognition, 2008. ICPR 2008. 19th International Conference*  
311 *on*, 1–4 (2008).
- 312 9 Q. Huang, Y. Luo, and Q. Zhang, “Breast ultrasound image segmentation: a survey.,” *Inter-*  
313 *national journal of computer assisted radiology and surgery* **12**(3), 493–507 (2017).
- 314 10 A. Alvarenga, A. Infantosi, W. Pereira, *et al.*, “Assessing the combined performance of tex-  
315 ture and morphological parameters in distinguishing breast tumors in ultrasound images,”  
316 *Medical Physics* **39**(12), 7350–7358 (2012).
- 317 11 B. Liu, H. Cheng, J. Huang, *et al.*, “Fully automatic and segmentation-robust classification  
318 of breast tumors based on local texture analysis of ultrasound images,” *Pattern Recognition*  
319 **43**(1), 280 – 298 (2010).
- 320 12 M. H. ”Yap, E. A. Edirisinghe, and H. E. Bez, “Object boundary detection in ultrasound  
321 images,” in *The 3rd Canadian Conference on Computer and Robot Vision (CRV’06)*, 53–53,  
322 IEEE (2006).
- 323 13 K. Drukker, N. P. Grusauskas, C. A. Sennett, *et al.*, “Breast US computer-aided diagnosis  
324 workstation: Performance with a large clinical diagnostic population,” *Radiology* **248**(2),  
325 392–397 (2008).
- 326 14 J. Shan, H. Cheng, and Y. Wang, “Completely automated segmentation approach for breast

- 327 ultrasound images using multiple-domain features,” *Ultrasound in Medicine and Biology*  
328 **38**(2), 262–275 (2012).
- 329 15 M. H. Yap, E. A. Edirisinghe, and H. E. Bez, “A novel algorithm for initial lesion detection  
330 in ultrasound breast images,” *Journal of Applied Clinical Medical Physics* **9**(4), 181–199  
331 (2008).
- 332 16 M. H. Yap, E. A. Edirisinghe, and H. E. Bez, “Fully automatic lesion boundary detection in  
333 ultrasound breast images,” (2007).
- 334 17 H. Shao, Y. Zhang, M. Xian, *et al.*, “A saliency model for automated tumor detection in breast  
335 ultrasound images,” 1424–1428 (2015).
- 336 18 L. Gao, W. Yang, Z. Liao, *et al.*, “Segmentation of ultrasonic breast tumors based on homo-  
337 geneous patch,” *Medical physics* **39**(6Part1), 3299–3318 (2012).
- 338 19 Z. Hao, Q. Wang, H. Ren, *et al.*, “Multiscale superpixel classification for tumor segmentation  
339 in breast ultrasound images,” in *Image Processing (ICIP), 2012 19th IEEE International*  
340 *Conference on*, 2817–2820, IEEE (2012).
- 341 20 L. Gao, X. Liu, and W. Chen, “Phase-and gvf-based level set segmentation of ultrasonic  
342 breast tumors,” *journal of applied Mathematics* **2012** (2012).
- 343 21 M. Xian, Y. Zhang, H. Cheng, *et al.*, “A benchmark for breast ultrasound image segmentation  
344 (buis),” *arXiv preprint arXiv:1801.03182* (2018).
- 345 22 W. Gomez, L. Leija, A. Alvarenga, *et al.*, “Computerized lesion segmentation of breast ultra-  
346 sound based on marker-controlled watershed transformation,” *Medical physics* **37**(1), 82–95  
347 (2010).

- 348 23 T. Prabhakar and S. Poonguzhali, “Automatic detection and classification of benign and ma-  
349 lignant lesions in breast ultrasound images using texture morphological and fractal features,”  
350 in *Biomedical Engineering International Conference (BMEiCON), 2017 10th*, 1–5, IEEE  
351 (2017).
- 352 24 Z. Hao, Q. Wang, Y. K. Seong, *et al.*, “Combining crf and multi-hypothesis detection for  
353 accurate lesion segmentation in breast sonograms,” in *International Conference on Medical  
354 Image Computing and Computer-Assisted Intervention*, 504–511, Springer (2012).
- 355 25 M. Xian, H. Cheng, and Y. Zhang, “A fully automatic breast ultrasound image segmenta-  
356 tion approach based on neutro-connectedness,” in *Pattern Recognition (ICPR), 2014 22nd  
357 International Conference on*, 2495–2500, IEEE (2014).
- 358 26 H. Cheng, J. Shan, W. Ju, *et al.*, “Automated breast cancer detection and classification using  
359 ultrasound images: A survey,” *Pattern Recognition* **43**(1), 299 – 317 (2010).
- 360 27 C. M. Sehgal, S. P. Weinstein, P. H. Arger, *et al.*, “A review of breast ultrasound,” *Journal of  
361 Mammary Gland Biology and Neoplasia* **11**(2), 113–123 (2006).
- 362 28 B. Sahiner, H.-P. Chan, M. A. Roubidoux, *et al.*, “Computerized characterization of breast  
363 masses on three-dimensional ultrasound volumes,” *Medical Physics* **31**(4), 744–754 (2004).
- 364 29 W. C. A. Pereira, A. V. Alvarenga, A. F. C. Infantosi, *et al.*, “A non-linear morphometric  
365 feature selection approach for breast tumor contour from ultrasonic images,” *Computers in  
366 Biology and Medicine* **40**(11), 912–918 (2010).
- 367 30 Y. Liu, H. Cheng, J. Huang, *et al.*, “Computer aided diagnosis system for breast cancer based  
368 on color doppler flow imaging,” *Journal of Medical Systems* **36**(6), 3975–3982 (2012).
- 369 31 M. H. Yap, E. Edirisinghe, and H. Bez, “Computer aided detection and recognition of lesions

- 370 in ultrasound breast images,” in *Innovations in Data Methodologies and Computational Al-*  
371 *gorithms for Medical Applications*, 125–152, IGI Global (2012).
- 372 32 M. H. Yap and C. H. Yap, “Breast ultrasound lesions classification: a performance evaluation  
373 between manual delineation and computer segmentation,” in *SPIE Medical Imaging*, 978718–  
374 978718, International Society for Optics and Photonics (2016).
- 375 33 G. Carneiro, J. Nascimento, and A. P. Bradley, “Unregistered multiview mammogram anal-  
376 ysis with pre-trained deep learning models,” in *International Conference on Medical Image*  
377 *Computing and Computer-Assisted Intervention*, 652–660, Springer (2015).
- 378 34 B. Huynh, K. Drukker, and M. Giger, “Computer-aided diagnosis of breast ultrasound images  
379 using transfer learning from deep convolutional neural networks,” *Medical Physics* **43**(6),  
380 3705–3705 (2016).
- 381 35 M. H. Yap, G. Pons, J. Mart, *et al.*, “Automated breast ultrasound lesions detection using con-  
382 volutional neural networks,” *IEEE Journal of Biomedical and Health Informatics* **22**, 1218–  
383 1226 (2018).
- 384 36 M. H. Yap, M. Goyal, F. Osman, *et al.*, “End-to-end breast ultrasound lesions recognition with  
385 a deep learning approach,” in *Medical Imaging 2018: Biomedical Applications in Molecular,*  
386 *Structural, and Functional Imaging*, **10578**, 1057819, International Society for Optics and  
387 Photonics (2018).
- 388 37 S. Prapavesis, B. Fornage, A. Palko, *et al.*, *Breast Ultrasound and US-Guided Interventional*  
389 *Techniques: A Multimedia Teaching File*, Thessaloniki, Greece (2003).
- 390 38 A. Garcia-Garcia, S. Orts-Escolano, S. Oprea, *et al.*, “A review on deep learning techniques  
391 applied to semantic segmentation,” *arXiv preprint arXiv:1704.06857* (2017).

- 392 39 M. Everingham, S. M. A. Eslami, L. Van Gool, *et al.*, “The pascal visual object classes  
393 challenge: A retrospective,” *International Journal of Computer Vision* **111**, 98–136 (2015).
- 394 40 M. Thoma, “A survey of semantic segmentation,” *arXiv preprint arXiv:1602.06541* (2016).
- 395 41 M. Goyal and M. H. Yap, “Multi-class semantic segmentation of skin lesions via fully con-  
396 volutional networks,” *arXiv preprint arXiv:1711.10449* (2017).
- 397 42 M. Goyal, M. H. Yap, N. D. Reeves, *et al.*, “Fully convolutional networks for diabetic foot ul-  
398 cer segmentation,” in *2017 IEEE International Conference on Systems, Man, and Cybernetics*  
399 *(SMC)*, 618–623 (2017).
- 400 43 M. Goyal, N. D. Reeves, A. K. Davison, *et al.*, “Dfunet: Convolutional neural networks for  
401 diabetic foot ulcer classification,” *arXiv preprint arXiv:1711.10448* (2017).
- 402 44 J. Long, E. Shelhamer, and T. Darrell, “Fully convolutional networks for semantic segmenta-  
403 tion,” in *Proceedings of the IEEE Conference on Computer Vision and Pattern Recognition*,  
404 3431–3440 (2015).
- 405 45 A. Krizhevsky, I. Sutskever, and G. E. Hinton, “Imagenet classification with deep convolu-  
406 tional neural networks,” in *Advances in neural information processing systems*, 1097–1105  
407 (2012).
- 408 46 Y. Jia, E. Shelhamer, J. Donahue, *et al.*, “Caffe: Convolutional architecture for fast feature  
409 embedding,” in *Proceedings of the 22nd ACM international conference on Multimedia*, 675–  
410 678, ACM (2014).
- 411 47 J. Duchi, E. Hazan, and Y. Singer, “Adaptive subgradient methods for online learning and  
412 stochastic optimization,” *Journal of Machine Learning Research* **12**(Jul), 2121–2159 (2011).

- 413 48 D. Zikic, Y. Ioannou, M. Brown, *et al.*, “Segmentation of brain tumor tissues with convolu-  
414 tional neural networks,” *Proceedings MICCAI-BRATS* , 36–39 (2014).
- 415 49 S. Pereira, A. Pinto, V. Alves, *et al.*, “Brain tumor segmentation using convolutional neural  
416 networks in mri images,” *IEEE Transactions on Medical Imaging* **35**(5), 1240–1251 (2016).
- 417 50 D. M. Powers, “Evaluation: from precision, recall and F-measure to ROC, informedness,  
418 markedness and correlation,” *Journal of Machine Learning Technologies* **2**, 37–63 (2011).
- 419 51 M. Everingham, L. Van Gool, C. K. Williams, *et al.*, “The pascal visual object classes (voc)  
420 challenge,” *International journal of computer vision* **88**(2), 303–338 (2010).

421 **Moi Hoon Yap** is Reader (Associate Professor) in Computer Vision at the Manchester Metropoli-  
422 tan University and a Royal Society Industry Fellow with Image Metrics Ltd. She received her  
423 Ph.D. in Computer Science from Loughborough University in 2009. After her Ph.D., she worked  
424 as Postdoctoral Research Assistant in the Centre for Visual Computing at the University of Brad-  
425 ford. She serves as an Associate Editor for Journal of Open Research Software and reviewers for  
426 IEEE transactions/journals (Image Processing, Multimedia, Cybernetics, biomedical health, and  
427 informatics).

428 **Manu Goyal** is a Research Scholar at the Manchester Metropolitan University. He received his  
429 Master of Technology in Computer Science and Applications from Thapar University, India. His  
430 research expertise is in medical imaging analysis, computer vision, deep learning, wireless sensor  
431 networks and internet of things.

432 **Fatima Mohamed Osman** is currently Secretary of the Board of Trustees of the World Organi-  
433 zation for Renaissance of Arabic Language, and a third year PhD student at Sudan University of



434 Science and Technology. She received her M.Sc. in Computer Science from University of Jordan,  
435 King Abdullah II School for Information Technology in Sep 2009. After her M.Sc. She served  
436 as a team member of Database Administration in IT Department at Zain Jordan Mobile Telecom  
437 (Jan 10 Dec 10). She worked as Teaching Assistant (Feb 2011 Nov 11) in the Department of  
438 Computer Science at the University of Africa.

439 **Robert Martí** is an associate professor at Computer Vision and Robotics Institute of the University  
440 Girona, Spain. He received his BS and MS degrees in Computer Science from the University  
441 of Girona in 1997 and 1999, respectively, and his PhD degree from the School of Information  
442 Systems at the University of East Anglia in 2003. He is the author of more than 30 international  
443 peer reviewed journal and 80 conference papers. His current research interests include machine  
444 learning and image registration applied to medical image analysis, computer aided diagnosis, and  
445 breast, prostate and brain imaging.

446 **Erika Denton** is a consultant radiologist in Norwich. Her appointment to the role of Associate  
447 Medical Director in 2016 is to provide leadership and strategic support to NNUHFT with specific  
448 responsibilities for working across the local STP footprint, with the UEA and to develop workforce  
449 and research strategies. In 2016 she was appointed to the role of Clinical Advisor in Imaging at  
450 NHS Improvement. This has included leading regional work with the Clinical Senate to review  
451 Interventional Radiology Services across the region.

452 **Arne Juette** is Consultant Radiologist and Ultrasound lead at Norfolk and Norwich University  
453 Hospital.

454 **Reyer Zwiggelaar** received the Ir. degree in Applied Physics from the State University Gronin-

455 gen, Groningen, The Netherlands, in 1989, and the Ph.D. degree in Electronic and Electrical En-  
456 gineering from University College London, London, UK, in 1993. He is currently a Professor  
457 in the Department of Computer Science, Aberystwyth University, UK. He is the author or co-  
458 author of more than 250 conference and journal papers. His current research interests include  
459 Medical Image Understanding, especially focusing on Mammographic and Prostate Data, Pattern  
460 Recognition, Statistical Methods, Texture-Based Segmentation, Biometrics, Manifold Learning  
461 and Feature-Detection Techniques. He is an Associate Editor of Pattern Recognition and Journal  
462 of Biomedical and Health Informatics (JBHI).

## 463 **List of Figures**

- 464 1 Illustration of some images from the datasets and its ground truth labeling in  
465 PASCAL-VOC format.(a) and (b) are images from Dataset A; (c) and (d) are im-  
466 ages from Dataset B; and index 1 (RED) indicates malignant lesion and index 2  
467 (GREEN) indicates benign lesion.
- 468 2 Overview of the semantic segmentation architecture.
- 469 3 Transfer learning procedure of deep CNNs to obtain optimized weights initializa-  
470 tions. Three fully connected layers of CNN were removed and replaced by three  
471 convolutional layers, making the pre-trained model fully convolutional.
- 472 4 The accuracy of the proposed methods when considering the number of images  
473 with *Dice* score  $> 0.5$ .

474 5 Visual comparison of the lesions segmentation and recognition with FCNs. The  
475 first column is the ground truth delineation, the second column is the proposed  
476 transfer learning FCN-AlexNet, the third column is the proposed transfer learning  
477 FCN-32s and the fourth column is the proposed transfer learning FCN-16s and the  
478 last column is the proposed transfer learning FCN-8s. The first and second rows  
479 showed the best case scenarios where the lesions were correctly segmented and  
480 classified. The third and fourth rows showed difficult cases where FCNs failed in  
481 those cases.

## 482 **List of Tables**

483 1 Summary of the performances for different lesion types for four semantic segmen-  
484 tation methods in *Mean*. *SD* is standard deviation.